Comparative Study of the MPPT Control for the Photovoltaic Water Pumping System between FSS-P&O and VSS-P&O

REHOUMA YOUSSEF[1,4,*], NAOUI MOHAMED[2,*], ROMDHANE BEN KHALIFA[3], TAIBI DJAMEL[1], GOUGUI ABDELMOUMEN[1], ABDERRAHMANE KHECHEKHOUCHE[5], SBITA LASSAAD[2]

[1]LAGE Laboratory,
University of Ouargla,
Ouargla,
ALGERIA

[2]Research Unit of Energy Processes Environment and Electrical Systems,
ENIG, University of Gabes,
Gabes,
TUNISIA

[3]Laboratoire de Mécanique Productique Et Énergétique (LR18ES01),
Université de Tunis - ENSIT,
Tunis,
TUNISIA

[4]LEVRES Laboratory,
University of EL Oued,
ALGERIA

[5]Faculty of Technology,
University of EL Oued,
ALGERIA

**Corresponding Authors*

Abstract: - This paper describes the implementation of a renewable energy system that operates independently. It comprises a photovoltaic generator (PV) that supplies power to a solar pumping system, driven by a permanent magnet direct current motor (PMDC) via a DC-DC Buck converter. Consequently, the objective is to maintain steady operation with continuous power supply despite changes in two environmental parameters, including solar irradiation and absolute temperature. The maximal power extraction of the PV panel using the usual perturbation and observation (P&O) technique achieves this objective. This method must provide appropriate duty cycle control for the DC-DC buck converter when the user-selected Fixed-Step Size (FSS) is used, unfortunately, selecting an insufficient fixed-step size led to a power ripple issue with the PV panel. Incorporating a new Variable Step-Size (VSS) into the traditional P&O algorithm shows the occurrence of the enhanced P&O-MPPT control approach. The proposed technique is validated by utilizing the PROTEUS/ISIS software. For various climatic situations, the results demonstrate that the proposed control technique is preferable to the one based on the standard P&O-MPPT.

Key-Words: - Photovoltaic system, pump, Proteus ISIS, Arduino, FSS-P&O, VSS-P&O.

Received: April 19, 2023. Revised: February 21, 2024. Accepted: April 24, 2024. Published: May 14, 2024.

1 Introduction

As Algeria is a developing nation, water supply and accessibility in various locations are hampered by the presence of numerous rural areas and variable weather conditions. In such situations, a solar water pumping system is an excellent alternative for

irrigation and other daily tasks, [1] , as it is highly reliable, requires less maintenance, and is simple to build, [2].

Renewable energies are ecologically and environmentally clean, unlike hydrocarbon fuels (oil, gas, and coal), making them the focus of social and industrial sectors, [3]. Solar photovoltaics, one of the renewable energies, are abundant on the planet's surface, simple to convert to direct power, adaptable, and do not require sophisticated mechanical parts that create noise during production, [4], [5]. To increase the performance of such systems, the Maximum PowerPoint Approach (MPPT), a control technique, must be implemented. The MPPT can monitor the MPP online despite changes in irradiance and temperature, [6], [7]. Numerous optimal tactics are implemented to enhance the performance of water pumping systems, among which the P&O control is the most prevalent. However, its effectiveness is modest, and its oscillations around the MPP are significant, [8].

Several solutions are implemented to facilitate the investigation of water pumping from the primary hand pump to high-efficiency electric pumps with less effort and energy. Diesel pumping is extensively investigated in remote locations without access to the electrical grid. However, this technique demands an expensive and environmentally damaging fuel supply. Consequently, several users have integrated PV energy for water pumping, [9], [10]. As with any system that utilizes solar radiation, the system's performance depends on weather conditions, seasonal fluctuations, [11], thermal qualities, module material attributes, and mounting structure, [12] .

Employing high-efficiency power trackers designed to harvest the most power feasible from the PV module can reduce the total system cost, [13], [14]. Numerous approaches for MPPTs have been consistently developed and enhanced. These techniques include perturb and observe (P&O) [15] , incremental conductance [16], hill climbing [17], [18], fractional open-circuit voltage, fractional short-circuit current, neural network, fuzzy logic control [19], [20] and genetic algorithms [21], [22]. These methods vary regarding the number of sensors necessary, their complexity cost, and their efficiency level, wobbling about the MPP, convergence speed, and rectifying tracking route when irradiance and temperature change.

In this context, the classic P&O approach (with fixed step size) is routinely employed in PV field applications, [7], [23], [24] because of its ease of implementation. The latter is determined by perturbing the PV output voltage and watching the resulting change in PV array power. This one analyses the effect of a perturbation in the PV output voltage on the PV array's power, [25], [26]. Multiple sensors are required for measuring the PV current and voltage. In addition to failing the peak power test, [27], [28], it exhibits instability in the steady-state regime, making it less precise and potentially causing energy loss when there are frequent and rapid variations in light. A small step size may be selected to prevent oscillations, even though this decision leads to a lengthy response time, [29]. Therefore, when selecting the increment, a trade-off between tracking speed and accuracy is evaluated, [30]. Several studies suggest VSS P&O algorithms, which are variants of the step size of the P&O technique, [31], to address the concerns mentioned above. In addition, a feedback PI controller is employed to reduce the difference between the reference and actual torque speed when these techniques are supported by speed control.

Our work aims to describe the design characteristics of a PMDC motor based on a photovoltaic pumping system using Proteus/Isis software. Additionally, this paper proposes a modified P&O MPPT algorithm to address the shortcomings of the standard P&O method when operating under varying weather conditions, thereby significantly improving the accuracy of the control system. Furthermore, the performance of the entire photovoltaic power system was enhanced by controlling the physical parameters, such as motor speed.

2 Connection Layout System

Figure 1 depicts the connection layout of the analyzed system. The modified water pumping system includes a DC-DC buck converter fed by a PV source, an MPPT-controlled PMDC motor, and a PWM switching mechanism. It is noteworthy that the MPPT controller is implemented on an Arduino board, which controls the buck converter and tracks the MPP using current and voltage data. The resulting power, current, and voltage of the photovoltaic panel are presented on the LCD screen.

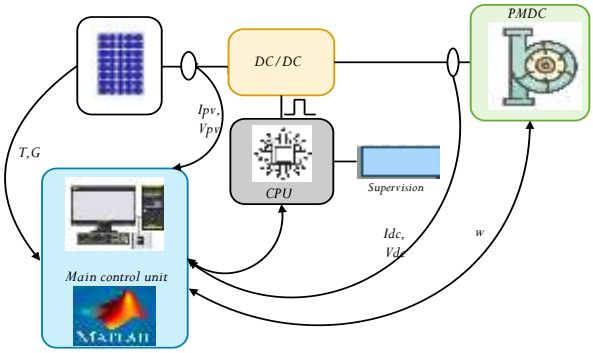

Fig. 1: Simplified diagram of the global system

2.1 PMDC Motor Model

The permanent magnet DC motor (PMDC motor) has been modeled in terms of both torque and rotor angle, [32], [33]. The PMDC motor model is developed using Proteus/ISIS software, as illustrated in Figure 2. The characteristic equations of a PMDC motor can be expressed as:

$$V = R_a I_a + L_a \frac{dI_a}{dt} + e \quad (1)$$

$$e = K_e w_m \quad (2)$$

$$T_e = K_t I_a = J \frac{dw_m}{dt} + B_m w_m + T_L \quad (3)$$

Where J denotes the moment of inertia, B_m is the friction torque factor, and T_L and T_e represent the load and electromagnetic torques, respectively. The model, however, is constructed using Equations (1), (2), and (3). Additionally, the PMDC motor block can be consolidated into a single block through simulation with the Proteus/Isis software.

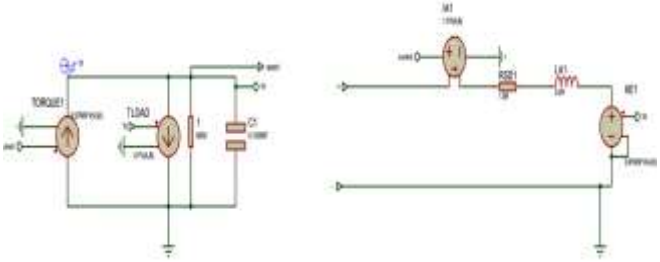

Fig. 2: Model of PMDC motor

2.2 Centrifugal Pump

Compared to other electric motors, a permanent magnet direct current (PMDC) motor is linked to a centrifugal pump and requires a comparatively small starting torque, [34]. The centrifugal pump's load torque is determined by:

$$T_L = A_l K_l \omega_m^{1.8} \quad (4)$$

Equation (4) has been implemented in Proteus to recreate the centrifugal pump. The modeling of a centrifugal pump is depicted in Figure 3. The pump is a subsystem with a single input and output terminal; ω_m is the input motor speed, and T_L is the output torque. Table 1 lists the technical parameters utilized in modeling the motor pump system.

Table 1. Parameters of PMDC motor, and Load pump data

Data of DC PM motor	
Voltage (Va) (rated)	160 V
Current (I a) (rated)	9.5 A
Speed (ω) (rated)	220 (rad .sec^{-1})
Resistance of armature (Ra)	0.15e-2 c
Inductance of armature (La)	0.2 H
Voltage constant (K e)	6.7609e-1 V/ (rad.sec^{-1})
Torque constant (KT)	6.7609e-1 N.m.A^{-1}
Motor friction (Am)	0.2 N m
Load pump data	
Inertia moment (J)	2.365e-2 K g.m^2
Viscous Friction factor (B)	2.387e-3 N.m/(rad.sec^{-1})
Load torque constant (Ke)	3.9e-4 N.m/(rad.sec^{-1})
Friction of load (Al)	0.3 N.m

2.3 Modeling the PV Panel Generator

This model is developed using mathematical formulae drawn from the equivalent circuit of a solar panel, [35], [36]. It consists of a photocurrent source, diode, shunt, and series resistors. This model is connected to an Arduino MEGA Board via sensors of current and voltage to maximize the power of the photovoltaic generator, [37]. Figure 4 depicts the PV model's implementation in Proteus.

The sensitivity of an Arduino-based control circuit in Maximum Power Point Tracking (MPPT) is critical for accurately and swiftly tracking the maximum power point (MPP) of a photovoltaic (PV) panel amidst changing environmental conditions. This sensitivity is influenced by several factors, including the resolution of sensors and Analog-to-Digital Converters (ADCs), as well as the effectiveness of the control algorithm. Higher resolutions in sensors and ADCs enable the detection of small changes in voltage and current, while a well-designed control algorithm promptly adjusts circuit parameters to track the MPP effectively. To enhance sensitivity, one can choose high-resolution sensors and ADCs, optimize control algorithms, or even consider using dedicated MPPT Integrated Circuits (ICs). Sensitivity is crucial in MPPT systems to ensure the PV panel consistently operates at its MPP, maximizing power output. This is particularly important in applications facing fluctuating environmental conditions, such as solar tracking or off-grid systems.

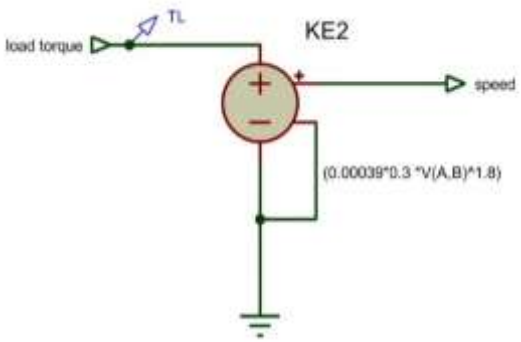

Fig. 3: Model of centrifugal pump

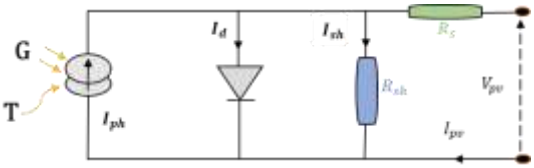

Fig. 4: Photovoltaic panel (Equivalent circuit)

A photovoltaic panel output current may be calculated using this model, as shown below, [35], [38]:

$$I_{pv} = I_{ph} - I_d - I_{sh} = I_{ph}N_p - N_p I_{sd}(e^{(\frac{V_{pv}+R_s I_{pv}}{n1 V_{th} N_s})} - 1) - N_p \frac{V_{pv}+RsI_{pv}}{N_s R_{sh}} \quad (5)$$

$$I_{ph} = (I_{sc} + k_i(T - 293.15))(\frac{G}{1000}) \quad (6)$$

$$I_{sd} = \frac{I_{sc}+k_i(T-293.15)}{e^{(\frac{q(V_{OC}+K_V)(T-293.15)}{\alpha K_T N_S})}-1} \quad (7)$$

Where Ipv, Iph, Ish, Id, and Isd denote the currents of: output, PV panel, shunt resistor, diode, and diode's reverse saturation, respectively, and Vpv is the output voltage. The manufacturer-supplied technical characteristics of the PV panel are listed in Table 2. A PV array is constructed by connecting four PV modules in series with two modules in parallel. The Ppv (Vpv) properties for various environmental inputs have been examined. Figure (5a) illustrates the Ppv (Vpv) curves for solar radiation ranging from 500 to 800 W/m² at a constant 25°C. Figure (5b) depicts the Ppv (Vpv) curves for temperatures ranging from 20 to 40°C and constant solar radiation of 1 kW/m².

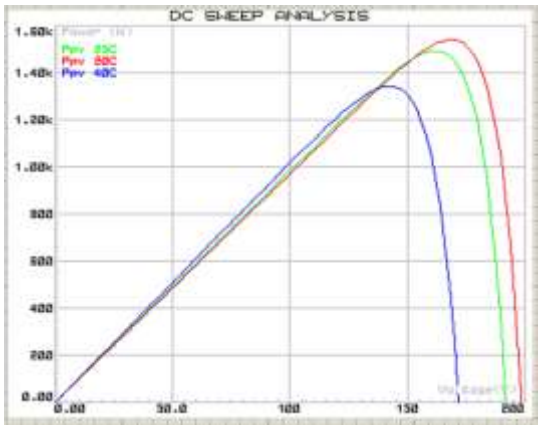

(a) Variable temperature

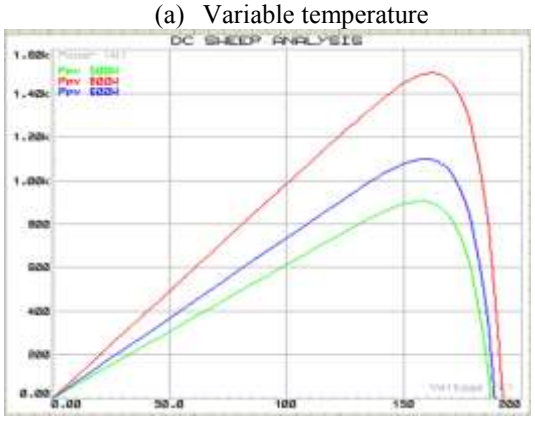

(b) Variable radiation

Fig. 5: Ppv (VPV) curves of the simulated module

Table 2. Technical data of the Canadian Solar CS6X-240P PV panel

Cell Type	Monocrystalline silicon	
Rated Power	Pmax	240W
The voltage at Maximum Power	Vpm	40.5 V
Current at Maximum Power	Ipm	5.93 A
Open Circuit Voltage	Vco	49.2 V
Short-Circuit Current	Icc	6.38 A
Module Efficiency	n	16.2 %
Temperature factor (open-circuit voltage)	Kv	-0.36901 mV/°C
Temperature factor (short-circuit current)	Ki	0.086998 mV/°C
NOCT	45 ± 2	°C
Dimensions	1640 x 992 x 40	mm
Weight	19.5	kg
Number of Cells	Ncell	72

A PV array is designed by connecting 4 PV modules in series and 2 modules in parallel.

2.4 Model of the Buck Converter

The Buck converter, as seen in Figure 6, is a DC-to-DC step-down converter. The adapter converter has been included in the proposed study because it has corresponding connection points on the adapter for increased lift, [39]. The duty cycle for the Buck converter is set at 100% conversion, a feature not achievable when using the boost converter.

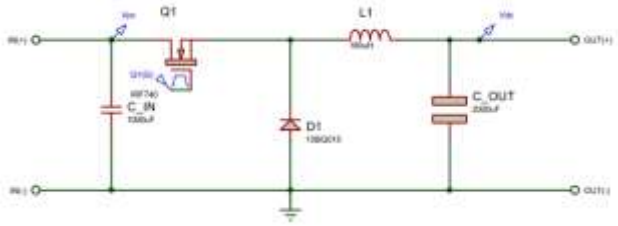

Fig. 6: DC-DC Buck Converter

The bidirectional converter runs in Buck mode when the switch Q1 and the diode D1 are conducting. In this circumstance, the battery is charged while the inductor current iL is negative.

The differential system models the buck mode converter mathematically.

$$\begin{cases} \frac{di_{L1}}{dt} = -\frac{u_1}{L1}V_{dc} + \frac{V_{pmdc}}{L1} - \frac{R}{L1}i_{L1} \\ i_{pmdc} = u_1 i_{L1} \end{cases} \quad (8)$$

With u1 = 1 if Q1 is closed and 0 otherwise.

2.5 Conventional Perturb and Observe MPPT Method

PV systems are recognized for their low efficiency and nonlinear nature, [40]. Additionally, PVs have a unique maximum power point (MPP). Due to the disadvantages mentioned above, monitoring the PV array's MPP is essential. Several MPPT strategies, such as Perturb and Observe (P&O) methods, [24], [41], [42], hill-climbing, and incremental conductance, [43], [44], [45], have been examined in the open literature. P&O with a constant step size has a basic structure and is easy to implement; hence, it is recognized among the most popular MPPT algorithms. Its central concept is based on the zero dP/dV values at the peak of the power-voltage curve. The P&O operates by perturbing (decreasing or increasing) the current or voltage of the PV array based on a comparison between the actual output power P(n) and that of the preceding perturbation P(n-1). Figure 7 depicts the recommended algorithmic flowchart for tracking the MPP. In this algorithm, the P&O method is utilized. First, the current and voltage of the solar generator are measured. Then, the output power of the solar generator may be determined. At time k, the photovoltaic power and voltage are compared to their values at time k-1. Lastly, the MPPT technique can be used to find the system reference speed that corresponds to output power maximization.

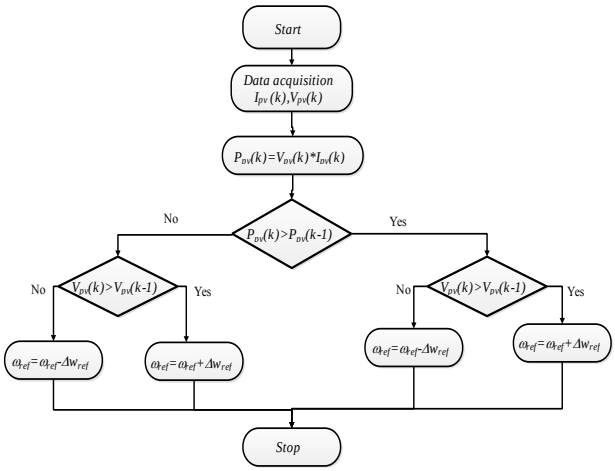

Fig.7: Flowcharts of standard P&O methods

2.6 Proposed Approach

This section will discuss the proposed supervision scheme for the solar pumping system. Any silicon device, such as a CPU or digital signal processor, can monitor the PV panel depicted in Proteus software, [46]. The combination of Arduino MEGA and ISIS Proteus software creates a compatible and effective photovoltaic pumping system. Figure 8 demonstrates that this system is also feasible in actual installations. Additionally, the control block is implemented in MATLAB/Simulink. PV electrical values are computed to determine PV characteristics (such as current and voltage). The control block serves as the system's backbone, primarily consisting of the Arduino MEGA board on which various MPPTs are implemented (P&O with fixed and variable step sizes).

The Arduino board is used to calculate the proper duty cycle, which is then sent to the MOSFET of the buck converter for control. In addition, the LCD screen is utilized to display electrical parameters for PV monitoring.

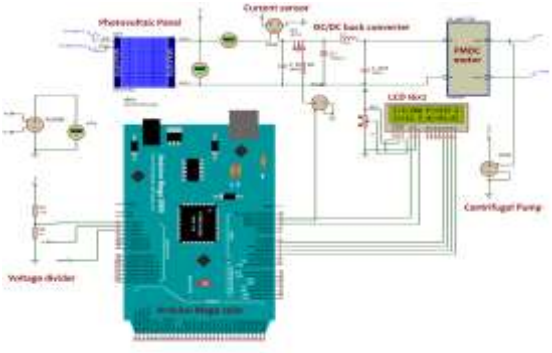

Fig. 8: Arduino-based control unit structure

2.7 Interfacing Arduino Mega2560 with MATLAB/ Simulink

Integrated Development Environment (IDE) is the essential programming software for the Arduino kit. IDE allows users to write programs, known as "Sketches," compile them, and then send them over USB to the Arduino board. This software environment is based on C/C++ programming languages and other open-source libraries. Additionally, this board can communicate with peripheral devices such as LCDs, sensors, and servo motors. However, many engineers find it challenging to program Arduino using C/C++ in real-world applications.

Consequently, the code is implemented differently in this paper. Instead of using Arduino IDE's script codes, Simulink enables the direct dragging and dropping of blocks onto the work environment with easy connections between them. The Arduino Support Package in Simulink is utilized to program the Arduino board. This package automates the transition from the Simulink model to the corresponding code, which the Arduino board can then efficiently execute. Figure 9 depicts the block diagram for Simulink, highlighting the entire Simulink model utilized in this study.

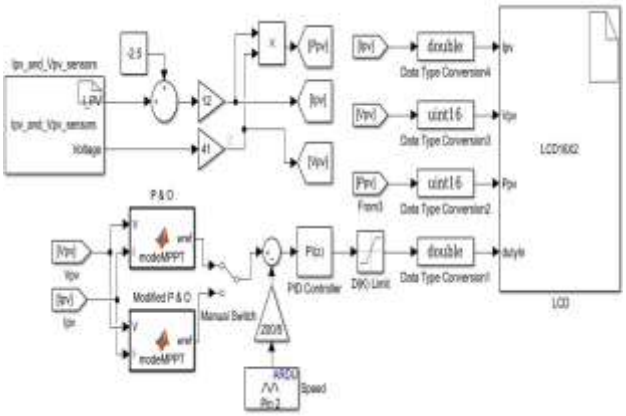

Fig. 9: Blocks of the Arduino package in MATLAB / Simulink

The supervision system is composed of three components:

Hardware input: In this subsystem, sensor data is initially received before being processed/utilized by software.

Control: The control signal to be transmitted to the Buck converter is computed using a two-stage process: (1) the selected MPPT algorithm calculates the reference speed, and (2) the proportional-integral (PI) controller attempts to minimize the error by comparing the reference speed to the actual motor speed. It is notable that in this section, to compare the MPPT algorithms, the Simulink model with manual switching is modified.

Hardware output: In this section, the Arduino board transmits the PWM (duty cycle) control signal to the Buck converter (simulated in Proteus). Additionally, the LCD panel will display the measurements (voltage, current, power, and duty cycle (%)). Moreover, all technical data will be transmitted to the Proteus software for real-time curve display.

2.8 Proposed (VSS) Perturb & The Algorithm

In the directly associated PV Water Pumping system (PVWPs), the PV array is directly coupled to the pump load without utilizing an optimization method (such as MPPT). Utilizing the P&O algorithm to track the MPP enhances the effectiveness of the PVWPS (fast-tracking and low oscillations). In the present method, the updated P&O algorithm calculates the step size based on the motor reference speed instead of the conventional voltage-based step. A specified reference step (denoted δωR) is multiplied by the power difference as an amplification factor. This method is helpful because it depends solely on the load's physical characteristics (the motor speed). By adopting this method, it is possible to avoid any modeling flaws that affect the input-output behavior. Figure 10 depicts the functional steps of the speed-based P&O algorithm.

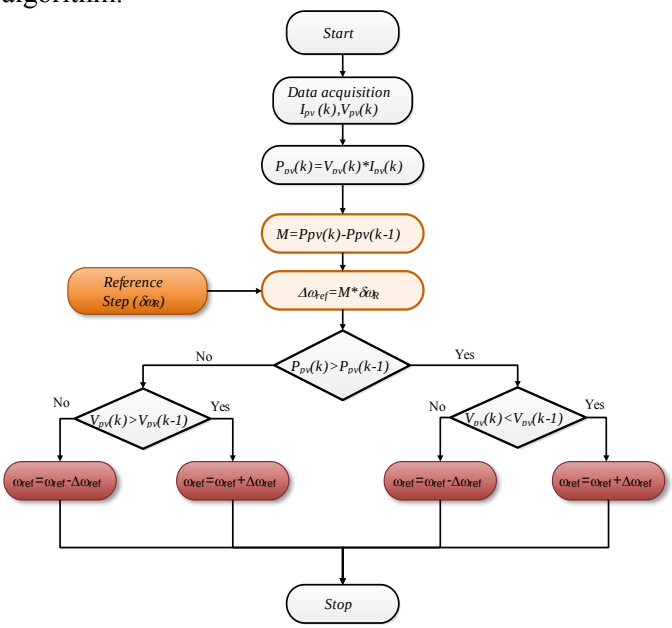

Fig. 10: Flowchart of the proposed (VSS) P&O

2.9 PI Control

Let ω_{ref} denotes the speed of reference delivered by the VSS MPPT algorithm. is the actual speed of the motor, the error ε is then written as:

$$\varepsilon = \omega_{ref} - \omega \quad (9)$$

The PI control signal is formulated as:

$$Control = K_p\varepsilon + K_i \int \varepsilon \quad (10)$$

Where K_p and K_i denotes the PI controller's gains (proportional and integral).

3 Results and Discussions

3.1. Comparison between VSS and FSS (P&O) under Constant Temperature and Radiation

A comparison of two MPPT techniques is conducted to validate the suggested method. In a photovoltaic pumping system, these strategies have been implemented. The latter does not require an electrochemical storage subsystem because it is powered by solar energy alone. Figure 11 and Table 3 provide a summary of the comparative results.

Figure 11 demonstrates that the P&O method with a step of 0.05 has better dynamic performance than the 0.005 step P&O algorithm; it can approach the steady state more quickly, but the oscillations therein are substantially higher. It takes 0.05 s to reach the MPP. However, the 0.005 step P&O takes 1 s to reach the MPP. A more significant step can further improve the P&O algorithm's dynamic performance. Despite this, static performance will suffer as a result. A P&O method with varying steps can prevent or mitigate these performance deficiencies (in both dynamic and steady-state regimes). Our method has eradicated the steady-state oscillations, and the PV generator's output power is at its maximum. Based on Table 3, it is evident that variable step-size P&O (P&O VSS) outperforms fixed step-size P&O (P&O FSS) for three solar radiation values (0.08 kW/m², 0.5 kW/m², and 0.4 kW/m²) with a sudden shift of maximum power reference (1.5174 kW, 0.9336 kW, and 0.7387 kW).

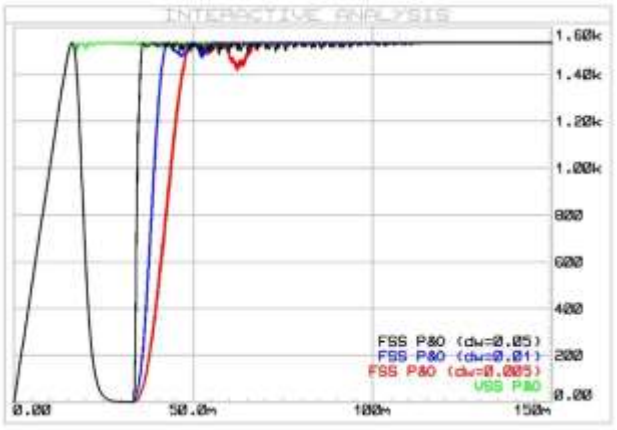

Fig. 11: Comparison of PV output power (Proposed VSS-P&O and FSS P&O)

The simulations were conducted under constant temperature (25°C) and illumination (800 W/m²). Additionally, distinct perturb steps (δω) have been implemented (0.005, 0.01, and 0.05). Figure 10 depicts the generated energy of the PV system. When the step size is increased, the FSS P&O approach yields superior response time results. Although the MPPT with an FSS of 0.05 minimizes response time, it causes more considerable oscillations in the steady state, which is detrimental to the MPPT's efficiency. The VSS P&O dynamic performance is superior to that of FSS P&O. Response time and steady-state oscillations of VSS P&O are superior to those of competing techniques.

Table 3. Comparison between P&O fixed & variable step-size techniques

MPPT Technique	Parameters	Irradiation G (W/m²)		
		800	500	400
FSS P&O	P_{max} (W)	1535	950.7	755.8
	P_{pv} (W)	1517.4	933.6482	738.7806
	Tracking Time (s)	0.036	0.0556	0.069
	Oscillation in Steady-state	High	High	High
	n_{MPPT}	0.9885	0.9821	0.9776
	R_{error}	0.0259	0.0348	0.0386
VSS P&O	P_{max} (W)	1541	955.6	758.4
	P_{pv} (W)	1528.8	944.9193	750.0007
	Tracking Time(s)	0.0162	0.026	0.032
	Steady-state oscillation	Minimized	Minimized	Minimized
	n_{MPPT}	0.9960	0.9939	0.9923
	R_{error}	0.0254	0.0336	0.0373

Additionally, using this method reduces both response time and static regime oscillations. Moreover, it achieves a significant efficiency of 99.60% and a tiny relative error in all examined circumstances. On the other hand, steady-state power oscillations are large, with a relative inaccuracy reaching 3.86 percent when using the classical method.

Climatic conditions, precisely the array temperature and incident solar energy, vary throughout the day. These variations differ significantly based on the examined zone. Consequently, two distinct scenarios are studied to evaluate the system's performance:

• Variable solar radiation profile and constant temperature

Regarding the power curve, the proposed solar radiation profile exhibits the same behavior as the PV system's power. As depicted in Figure 12, the value of solar irradiation decreases in the intervals [0 sec, 6 sec] and [8 sec, 10 sec], and increases in the interval [6 sec, 8 sec] to evaluate the algorithm's sensitivity. During periods of transitional irradiance, the PV system's power closely follows the MPP.

(a) Solar radiation profile

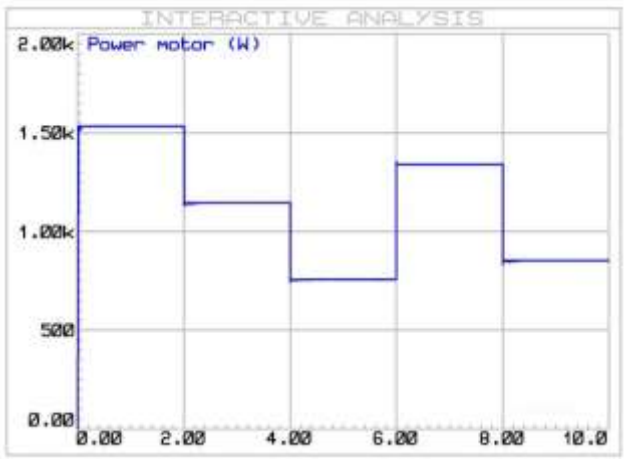

(b) Motor Power

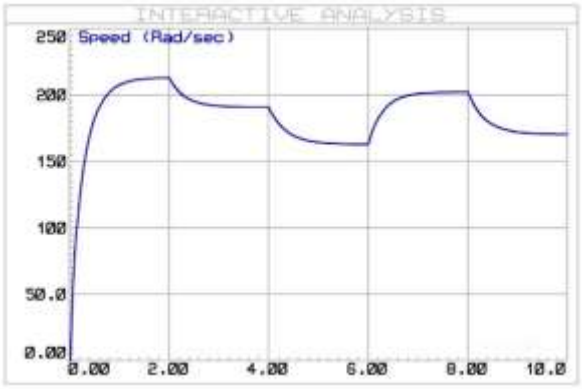

(c) Rotor speed

(d) Load torque

Fig. 12: Results of PMDC Power motor, Speed, and load torque characteristic at MPPT connected PV system for constant temperature and variable irradiation.

•Variable temperature profile and constant solar radiation

In this instance, a sudden temperature change from 20°C to 40°C is applied. Figure 13 depicts the temperature-dependent simulation findings. In this simulation, a constant solar radiation parameter of 0.8 kW/m² has been employed. The switching frequency of buck converters is inversely related to temperature. Additionally, when this value drops, the motor's rotational speed increases. In contrast, as the temperature decreases, the PV power rises, leading to an increase in the flow rate, and consequently, meeting the daily water pumping requirement. It has been determined that their performances diminish as the temperature rises.

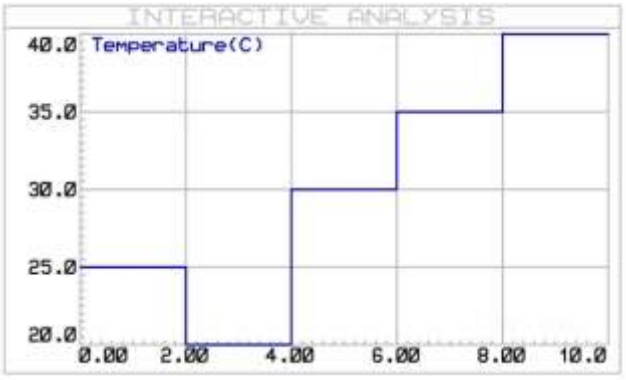

(a) Temperature profile

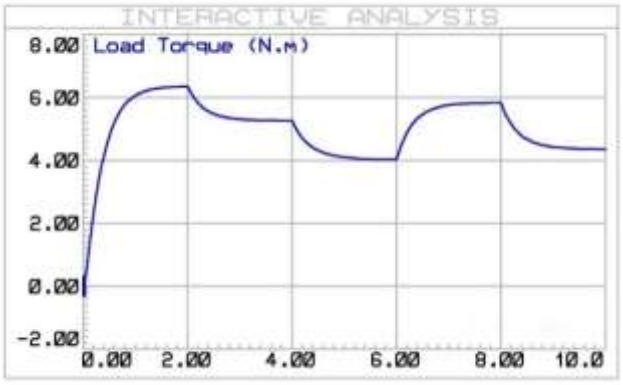

(b) Motor Power

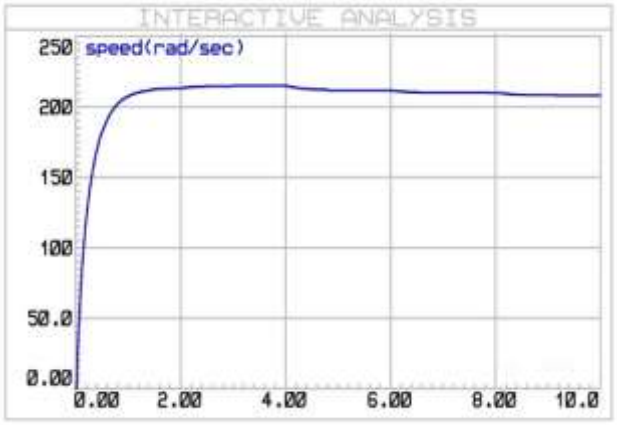

(c) Rotor speed

(d) Load torque

Fig. 13: Results for 0.8 kW/m^2 and variable temperature with VSS - P&O MPPT controller

3.2 Discussions and Statistic

When comparing the P&O with FSS equal to 0.01 and the P&O with FSS equivalent to 0.05, it is evident that the latter offers a dynamic performance that is relatively adequate; it can swiftly converge to the steady-state regime, albeit with more significant oscillations. The two examples above demonstrate that our methodology is more advantageous to the water pumping system than the conventional method. These scenarios replicate the natural environment in terms of fluctuating temperature and solar radiation, allowing a more thorough performance evaluation. According to Figure 12 and Figure 13, the abrupt change in environmental circumstances has a negligible impact on the performance and efficiency of the system. These findings demonstrate that our method can identify the optimal performance for each environmental change by modifying the MPP search. Additionally, by using speed-based P&O, the performance in terms of rotor speed stability is significantly enhanced, mainly due to the elimination of voltage modeling flaws. Table 4 outlines the primary characteristics of the various MPPT algorithms. These algorithms were assessed and compared based on their technical knowledge of PV panel parameters, complexity, speed, and precision.

Table 4. MPPT techniques employed (Comparison)

MPPT Algorithms	FSS P&O	VSS P&O	INC	FCO	FCC	LF
The type of sensors used	Voltage Current	Voltage Current	Voltage Current	Voltage	Current	Current
Identification of PV panel parameters	Not necessary	Not necessary	Not necessary	yes necessary	yes necessary	yes necessary
Complexity	low	low	mean	very low	very low	high
Number of iterations	41	36	48	35	41	27
Convergence speed	fast	fast	mean	fast	fast	very fast
Precision	98.85%	99.6%	97%	94%	94%	99%

The two proposed techniques are compared in Figure 14. This diagram displays five components that comprise the efficiency parameter, which is determined using the preceding relationship and simulation outcome. According to the literature, the simple MPPT is the most commonly used; nevertheless, when compared to the MPPT FSS and VSS, the expected overall energy performance is lower than that observed. Based on these findings, it is clear that this type of algorithm affects overall

performance and can either increase or decrease the use of this technology to power the solar pumping system.

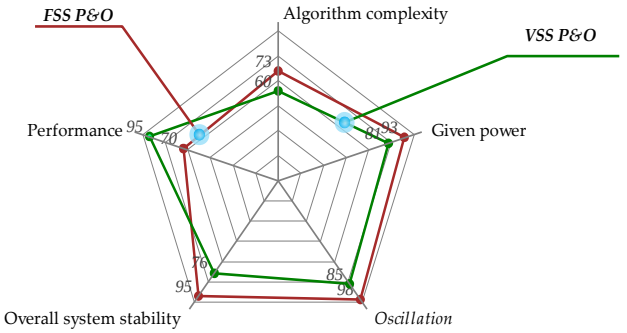

Fig. 14: The comparison between FSS and VSS MPPT

4 Conclusion

This paper examines photovoltaic pumping systems without the need for a battery bank. Two MPPT algorithms have been implemented (P&O with fixed and variable step sizes). We employed interactions between the Proteus/Isis and MATLAB/Simulink simulation platforms to track the MPP by providing the ideal motor speed as a reference. The latter is evaluated with a varied torque load. This method reinforces the PWM computation strategy by the motor speed reference value, which the proportional-integral controller subsequently governs. The proposed method minimizes the P&O method's response time and dynamic error when implemented. With varying temperature and irradiance profiles, the suggested approach, with its simple structure, has obtained improved results with minimum divergence around MPPs and without additional hardware. Additionally, the new tracker achieves high dynamic efficiency with an acceptable oscillation level during the steady-state phase. It has been demonstrated that 0.05 is the optimal step size for the VSS P&O. In typical settings, our algorithm is 99.6% more efficient. Future studies will evaluate the suggested approach under a partial shade scenario. Additionally, it is possible to validate it with different sorts of converters.

References:

[1] B.Bouzidi and P.E.Campana, "Optimization of photovoltaic water pumping systems for date palm irrigation in the Saharan regions of Algeria: increasing economic viability with multiple-crop irrigation," *Energy, Ecol. Environ.*, vol. 6, no. 4, pp. 316–343, 2021, https://doi.org/10.1007/s40974-020-00195-x.

[2] A. EISSA, M. F. El-Khatib, and M. I. A. El-Sebah, "Dynamics Analysis and Control of a Two-Link Manipulator," *WSEAS Transactions on Systems and Control*, vol. 18, pp. 487–497, 2023, https://doi.org/10.37394/23203.2023.18.52.

[3] R. R. Moussa, M. M. M. Mansour, and N. M. Yossif, "Statistic equation to estimate the amount of CO2 emission produced from high traffic density roads," *WSEAS Transactions on Power Systems*, vol. 16, pp. 78–86, 2021, https://doi.org/10.37394/232016.2021.16.8.

[4] S. Dubey, J. N. Sarvaiya, and B. Seshadri, "Temperature dependent photovoltaic (PV) efficiency and its effect on PV production in the world–a review," *Energy procedia*, vol. 33, no. 1, pp. 311–321, 2013, https://doi.org/10.1016/j.egypro.2013.05.072.

[5] K. Tsiakmakis, V. Delimaras, A. T. Hatzopoulos, and M. S. Papadopoulou, "Displacement Measurement System and Control of Ionic Polymer Metal Composite Actuator," *WSEAS Transactions on Systems and Control*, vol. 18, pp. 144–153, 2023, https://doi.org/10.37394/23203.2023.18.15.

[6] R. Sharma, S. Sharma, and S. Tiwari, "Design optimization of solar PV water pumping system," *Mater. Today Proc.*, vol. 21, , no. 3,pp. 1673–1679, 2020, https://doi.org/10.1016/j.matpr.2019.11.322.

[7] M. Kumar, K. P. Panda, J. C. Rosas-Caro, A. Valderrabano-Gonzalez, and G. Panda, "Comprehensive review of conventional and emerging maximum power point tracking algorithms for uniformly and partially shaded solar photovoltaic systems," *IEEE Access*,vol. 11,pp. 31778 - 31812 2023, https://doi.org/10.1109/ACCESS.2023.3262502.

[8] M. A. Eltawil, A. M. Alamri, and M. M. Azam, "Design a novel air to water pressure amplifier powered by PV system for reverse osmosis desalination," *Renew. Sustain. Energy Rev.*, vol. 160, p. 112295, 2022, https://doi.org/10.1016/j.rser.2022.112295.

[9] E. A. Ebrahim, "Real-Time Implementation of BLDC Motor-Based Intelligent Tracking Control Fed from PV-Array for E-Bike Applications", *WSEAS Transactions on Power Systems, vol 18,* pp. 270–281,*2023,* https://doi.org/10.37394/232016.2023.18.28.

[10] T.Ahmad, H.Zhu, D.Zhang, R.Tariq, A.Bassam, F.Ullah, A.S.AlGhamdi and S.S.Alshamrani, "Energetics systems and artificial intelligence: applications of industry

4.0" *Energy Reports*, vol. 8, p. 334-361, 2022, https://doi.org/10.1016/j.egyr.2021.11.256.

[11] A. Khechekhouche, A. Boukhari, Z. Driss, and N. Benhissen, "Seasonal effect on solar distillation in the El-Oued region of south-east Algeria," *Int. J. Energ.*, vol. 2, no. 1, pp. 42–45, 2017.

[12] A. M. Eltamaly, "A novel musical chairs algorithm applied for MPPT of PV systems," *Renew. Sustain. Energy Rev.*, vol. 146, pp. 111135, 2021, https://doi.org/10.1016/j.rser.2021.111135.

[13] S. Hakim, M. Elyaqouti, S. Farhat, L. Bouhouch, and A. Moudden, "Comparison of MPPT techniques:'P&O' and 'InCd' for PV systems," *Front. Sci. Eng.*, vol. 5, no. 2, pp. 7–13,2015, https://doi.org/10.34874/IMIST.PRSM/fsejournal-v5i2.28455.

[14] E. Rajendran, V. Raji, and V. K. D. Prabu, "Power Quality Acquire of Intelligent Controller based Superior Gain Re-Lift Luo Converter Intended for PV Linked Microgrid Integration," *WSEAS Transactions on Power Systems*, vol. 19, pp. 1–10, 2024, https://doi.org/10.37394/232016.2024.19.1.

[15] V. D. Gil-Vera and C. Quintero-López, "Predictive Modeling of Photovoltaic Solar Power Generation," *WSEAS Transactions on Power Systems*, vol. 18, pp. 71–81, 2023, https://doi.org/10.37394/232016.2023.18.8.

[16] N. A. Kamarzaman and C. W. Tan, "A comprehensive review of maximum power point tracking algorithms for photovoltaic systems," *Renew. Sustain. Energy Rev.*, vol. 37, pp. 585–598, 2014, https://doi.org/10.1016/j.rser.2014.05.045.

[17] M. I. Bahari, P. Tarassodi, Y. M. Naeini, A. K. Khalilabad, and P. Shirazi, "Modeling and simulation of hill climbing MPPT algorithm for photovoltaic application," in *2016 International Symposium on Power Electronics, Electrical Drives, Automation and Motion (SPEEDAM)*, *Capri, Italy,* 2016, pp. 1041–1044, https://doi.org/10.1109/SPEEDAM.2016.7525990.

[18] -B. Bekker and H. J. Beukes, "Finding an optimal PV panel maximum power point tracking method," in *2004 IEEE Africon. 7th Africon Conference in Africa (IEEE Cat. No. 04CH37590)*, *Gaborone, Botswana,* 2004, vol. 2, pp. 1125–1129, https://doi.org/10.1109/AFRICON.2004.1406864.

[19] S. Pan, Y. Li, S. PAN, and C. Lin, "Maximum Power Point Tracking Algorithm with Turn Round Measurement and Curve Fitting Method for Solar Generation System," *WSEAS Transactions on Circuits and Systems*, vol. 16, pp. 101–107, 2017.

[20] S. Hadji, J.-P. Gaubert, and F. Krim, "Theoretical and experimental analysis of genetic algorithms based MPPT for PV systems," *Energy Procedia*, vol. 74, pp. 772–787, 2015, https://doi.org/10.1016/j.egypro.2015.07.813.

[21] S. Hadji, J.-P. Gaubert, and F. Krim, "Real-time genetic algorithms-based MPPT: study and comparison (theoretical an experimental) with conventional methods," *Energies*, vol. 11, no. 2, pp. 459, 2018, https://doi.org/10.3390/en11020459.

[22] S. S. Chandel, M. N. Naik, and R. Chandel, "Review of solar photovoltaic water pumping system technology for irrigation and community drinking water supplies," *Renew. Sustain. Energy Rev.*, vol. 49, pp. 1084–1099, 2015, https://doi.org/10.1016/j.rser.2015.04.083.

[23] S. Messalti, A. Harrag, and A. Loukriz, "A new variable step size neural networks MPPT controller: Review, simulation and hardware implementation," *Renew. Sustain. Energy Rev.*, vol. 68, no.1, pp. 221–233, 2017, https://doi.org/10.1016/j.rser.2016.09.131.

[24] R. Youssef, M. A. Hamida, N. Mohamed, S. Lassaad, T. Djamel, and A. Yasmine, "Single-Stage Standalone Photovoltaic Water Pumping System Using Predictive Torque Control (PTC) of Induction Machine," *Electr. Power Components Syst.*, vol. 15, no. 5,pp. 1–17, 2023, https://doi.org/10.1080/15325008.2023.2278624.

[25] R. Gammoudi, H. Brahmi, and O. Hasnaoui, "Developed and STM implementation of modified P&O MPPT technique for a PV system over sun," *EPE J.*, vol. 29, no. 3, pp. 99–119, 2019, https://doi.org/10.1080/09398368.2018.1548804.

[26] K.-H. Chao, Y.-S. Lin, and U.-D. Lai, "Improved particle swarm optimization for maximum power point tracking in photovoltaic module arrays," *Appl. Energy*, vol. 158, pp. 609–618, 2015, https://doi.org/10.1016/j.apenergy.2015.08.047.

[27] O. B. H. B. Kechiche and H. Sammouda,

"Concentrator Photovoltaic System (CPV): Maximum Power Point Techniques (MPPT) Design and Performance," in *Solar Radiation-Measurement, Modeling and Forecasting Techniques for Photovoltaic Solar Energy Applications*, IntechOpen, pp. 1-18,2021, https://doi.org/10.5772/intechopen.98332.

[28] S. S. Kumar and C. Nagarajan, "Global Maximum Power Point Tracking (MPPT) Technique in DC–DC Boost Converter Solar Photovoltaic Array Under Partially Shaded Condition," *WSEAS Transactions on Power Systems*, vol. 12, pp. 49–62, 2017.

[29] Y. Jiang, J. A. A. Qahouq, and T. A. Haskew, "Adaptive step size with adaptive-perturbation-frequency digital MPPT controller for a single-sensor photovoltaic solar system," *IEEE Trans. power Electron.*, vol. 28, no. 7, pp. 3195–3205, 2012, https://doi.org/10.1109/TPEL.2012.2220158.

[30] R. A. Maher, A. K. Abdelsalam, Y. G. Dessouky, and A. Nouman, "High performance state-flow based MPPT technique for micro WECS," *IET Renew. Power Gener.*, vol. 13, no. 16, pp. 3009–3021, 2019, https://doi.org/10.1049/iet-rpg.2019.0157.

[31] A.-R. Youssef, H. H. H. Mousa, and E. E. M. Mohamed, "Development of self-adaptive P&O MPPT algorithm for wind generation systems with concentrated search area," *Renew. Energy*, vol. 154, pp. 875–893, 2020, https://doi.org/10.1016/j.renene.2020.03.050.

[32] C. A. Pérez-Gómez, J. Liceaga-Castro, and I. Siller-Alcalá, "Hard dead zone and friction modeling and identification of a permanent magnet DC motor non-linear model," *WSEAS Transactions on Systems and Control*, vol. 15, pp. 527–536, 2020, https://doi.org/10.37394/23203.2020.15.51.

[33] M. Ahmed Baba, M. Naoui, and M. Cherkaoui, "Fault-Tolerant Control Strategy for Hall Sensors in BLDC Motor Drive for Electric Vehicle Applications," *Sustainability*, vol. 15, no. 13, p. 10430, 2023, https://doi.org/10.3390/su151310430.

[34] S. Pant and R. P. Saini, "Solar water pumping system modelling and analysis using MATLAB/Simulink," in *2020 IEEE Students Conference on Engineering & Systems (SCES), Prayagraj, India,* 2020, pp. 1–6, https://doi.org/10.1109/SCES50439.2020.9236716.

[35] A. Gougui, "Comparison Study Between Improved JAYA and Particle Swarm Optimization PSO Algorithms for Parameter Extraction of Photovoltaic Module Based on Experimental Test," *Artif. Intell. Renewables Towar. an Energy Transit., Tipaza, Algeria*, vol. 174, p. 210, 2020, https://doi.org/10.1007/978-3-030-63846-7_21.

[36] M. B. Danoune, A. Djafour, Y. Rehouma, A. Degla, and Z. Driss, "Effective Modeling of Photovoltaic Modules Using Sailfish Optimizer," *Int. J. Energ.*, vol. 7, pp. 26–32, 2022.

[37] S. Motahhir, A. Chalh, A. El Ghzizal, and A. Derouich, "Development of a low-cost PV system using an improved INC algorithm and a PV panel Proteus model," *J. Clean. Prod.*, vol. 204, pp. 355–365, 2018, https://doi.org/10.1016/j.jclepro.2018.08.246.

[38] S. Li, W.Gong, X.Yan, C.Hu, D.Bai, L.Wang, and L.Gao, "Parameter extraction of photovoltaic models using an improved teaching-learning-based optimization," *Energy Convers. Manag.*, vol. 186, pp. 293–305, 2019, https://doi.org/10.1016/j.enconman.2019.02.048.

[39] F. A. Himmelstoss, "Design of State-Space Controllers with the Help of Signal Flow Graphs Shown for a Buck Converter," *WSEAS Transactions on Systems*, vol. 21, pp. 421–429, 2022, https://doi.org/10.37394/23202.2022.21.46.

[40] J. G. Shankar, J. B. Edward, and E. Neeraja, "Performance evaluation of a nine level cascaded multilevel inverter with single DC source for photovoltaic system," in *2017 Innovations in Power and Advanced Computing Technologies (i-PACT), Vellore, India,* 2017, pp. 1–8, https://doi.org/10.1109/IPACT.2017.8245215.

[41] N. Femia, G. Petrone, G. Spagnuolo, and M. Vitelli, "A technique for improving P&O MPPT performances of double-stage grid-connected photovoltaic systems," *IEEE Trans. Ind. Electron.*, vol. 56, no. 11, pp. 4473–4482, 2009, https://doi.org/10.1109/TIE.2009.2029589.

[42] V. R. Kolluru, S. S. Sarode, R. K. Patjoshi, K. Mahapatra, and B. Subudhi, "Design and implementation of an optimized sliding mode controller and compared with a conventional MPPT controller for a solar system," *WSEAS Transactions on Systems and Control*, vol. 9, no. 1, pp. 558–565, 2014.

[43] A. R. Reisi, M. H. Moradi, and S. Jamasb,

"Classification and comparison of maximum power point tracking techniques for photovoltaic system: A review," *Renew. Sustain. energy Rev.*, vol. 19, pp. 433–443, 2013, https://doi.org/10.1016/j.rser.2012.11.052.

[44] A. Safari and S. Mekhilef, "Simulation and hardware implementation of incremental conductance MPPT with direct control method using cuk converter," *IEEE Trans. Ind. Electron.*, vol. 58, no. 4, pp. 1154–1161, 2010, https://doi.org/10.1109/TIE.2010.2048834.

[45] L. Liqun and W. Zhixin, "A variable voltage MPPT control method for photovoltaic generation system," *WSEAS Transactions on Circuits and Systems*, vol. 8, no. 4, pp. 335–349, 2009.

[46] S. J. Yaqoob and A. A. Obed, "Modeling, simulation and implementation of PV system by proteus based on two-diode model," *J. Tech.*, vol. 1, no. 1, pp. 39–51, 2019, https://doi.org/10.51173/jt.v1i1.43.

Contribution of Individual Authors to the Creation of a Scientific Article (Ghostwriting Policy)

The authors equally contributed in the present research, at all stages from the formulation of the problem to the final findings and solution.

Sources of Funding for Research Presented in a Scientific Article or Scientific Article Itself

No funding was received for conducting this study.

Conflict of Interest

The authors have no conflicts of interest to declare.